Rheology and Ultrasound Scattering from Aggregated Red Cell Suspensions in Shear Flow

L. Haider,* P. Snabre,† and M. Boynard*

*Groupe de Recherche en Physique et Biophysique, 75270 Paris Cedex 06, France; and †Centre de Recherche Paul Pascal, CNRS UPR 8241, F33600 Pessac, France

ABSTRACT The shear flow dynamics of reversible red cell aggregates in dense suspensions were investigated by ultrasound scattering, to study the shear disruption processes of Rayleigh clusters and examine the effective mean field approximation used in microrheological models. In a first section, a rheo-acoustical model, in the Rayleigh scattering regime, is proposed to describe the shear stress dependence of the low frequency scattered power in relation to structural parameters. The fractal scattering regime characterizing the anisotropic scattering from flocs of size larger than the ultrasound wavelength is further discussed. In the second section, we report flow-dependent changes in the low-frequency scattering coefficient in a plane-plane flow geometry to analyze the shear disruption processes of hardened or deformable red cell aggregates in neutral dextran polymer solution. Rheo-acoustical experiments are examined on the basis of the rheo-acoustical model and the effective medium approximation. The ability of ultrasound scattering technique to determine the critical disaggregation shear stress and to give quantitative information on particle surface adhesive energy is analyzed. Lastly, the shear-thinning behavior of weakly aggregated hardened or deformable red cells is described.

INTRODUCTION

There is growing interest in the use of ultrasound scattering as a basis for nondestructive evaluation of media that consist of a homogeneous isotropic continuous phase in which small particles are randomly dispersed. The continuous phase may be liquid, with liquid or solid particles such as those found in food products, paints, lubricants, or biological systems. Significant progress has been made in recent years and was the subject of important practical interest for technological applications in many industrial fields, especially in biomedical areas (Greenleaf and Chandra, 1992; Greenleaf, 1996). Basic or applied research has been devoted to gaining fundamental knowledge of ultrasound-tissue interactions and quantitative tissue characterization (Greenleaf and Chandra, 1992). Much attention has been given to a better understanding of ultrasonic scattering processes in soft biological tissues and applying scattering methods to tissue characterization (Shung and Thieme, 1993; Greenleaf, 1996). However, ultrasonic wave propagation in soft tissues like liver, heart, kidney, or blood remains complex and involves several factors such as the acoustic impedance, compressibility, and density of the scatterer and the surrounding medium, as well as the space distribution and length scale of the scattering inhomogeneities (Greenleaf and Chandra, 1992; Shung and Thieme, 1993; Greenleaf, 1996).

The ultrasound scattering technique provides a way to investigate the rheological properties of suspensions and especially to characterize red cell aggregation processes and the structure of aggregates because the flocs are usually much smaller than the ultrasound wavelength, and Rayleigh scattering theory can be used. In the Rayleigh scattering regime, the low-frequency scattered power from a single aggregate scales as the square of the cluster volume (Rayleigh, 1945). However, both the internal structure of porous clusters and coherence effects may affect scattering from suspensions (Twersky, 1962, 1978, 1987; Mo and Cobbold, 1993). Over the last two decades, numerous theoretical models of ultrasound scattering from blood have been proposed and most have stemmed from research in either arterial disease assessment or hematology (Mo and Cobbold, 1993). The general goal in the former is to use Doppler ultrasound to evaluate the severity of arterial stenoses, which usually entails spectral analysis of the backscattered Doppler signal from the artery (Mo and Cobbold, 1993). In hematology, the main objectives are to control blood flow and evaluate the importance of red cell aggregation (Hanss and Boynard, 1979; Boynard and Lelievre, 1990; Cloutier and Qin, 1997). Most recent contributions focused on understanding the relationship between the ultrasonic scattered power and the particle volume fraction under different flow conditions (Lucas and Twersky, 1987; Shung et al., 1992). Little attention has been paid to the ultrasound scattering from a dense distribution of clusters, and most experimental work is still empirical (Lucas and Twersky, 1987; Yuan and Shung, 1988; Shung et al., 1992) because multiple hydrodynamic interactions in highly concentrated systems affect both floc size and ultrasonic scattered power.

Moreover, the non-Newtonian behavior of weakly aggregated suspensions results from the rupture of clusters when the shear stress is increased. Over the last 40 years, structural microrheological models involving an effective volume fraction and a shear-dependent structure parameter

Submitted February 17, 2004, and accepted for publication June 21, 2004.

Address reprint requests to M. Boynard, E-mail: michel.boynard@univ-paris5.fr.

0006-3495/04/10/2322/13 $2.00

doi: 10.1529/biophysj.104.041665

have been developed (Krieger, 1972; Quemada, 1978, 1998, 1999). Several authors have introduced the concept of fractal aggregation (Kolb and Jullien, 1984; Jullien and Botet, 1987). Mean field theories of growth and rupture of fractal clusters show a power law dependence of the viscosity on the shear rate (Mills, 1985; Sonntag and Russel, 1987; Mills and Snabre, 1988; Patel and Russel, 1988; Potanin and Uriev, 1991; Wessel and Ball, 1992; Potanin et al., 1995; Wolthers et al., 1996; Snabre and Mills, 1996) and usually consider the effective medium approximation that states that interacting clusters behave like isolate aggregates in a fluid whose viscosity is equal to the shear viscosity of the suspension. Computer simulations further suggest that the shear stress dependence of the equilibrium radius of clusters in a shear field is governed by a scaling power law (Potanin, 1993). However, little is known about the exact form of this scaling law that depends on the reversibility of cluster deformation under the action of external stresses.

In this article, the dynamics of reversible fractal clusters in dense suspensions was investigated by ultrasound scattering to analyze the shear break-up processes of fractal aggregates in dense suspensions, and further examine the effective mean field approximation used in microrheological models. For this purpose, we consider non-Brownian particles or aggregates smaller than the ultrasound wavelength, with acoustic properties close to those of the surrounding liquid, so that the attenuation of the coherent incident wave could be assumed to remain negligible, and multiple scattering could be ignored. On the basis of these assumptions, the hydrodynamic effects predominate over Brownian motion, and the Rayleigh scattering theory can then be used to estimate the single scattered incoherent intensity from a dilute random suspension. In highly packed systems, particles or clusters can no longer be considered as independent, and the correlation effects influence the ultrasonic scattered power because of wavelet interference in a dense distribution of scatterers (Twersky, 1962). The scattered power can be considered as the result of imperfect wave destruction, combined with either a packing factor (Twersky, 1987) or with the variance in the local scatterer concentration (Angelson, 1980; Mo and Cobbold, 1992).

The first section of this work mainly concerns ultrasound scattering from a dense suspension of fractal aggregates smaller than the ultrasound wavelength. On the basis of the hybrid approach, a first-order expression of the ultrasound scattering cross-sectional area per unit of volume for a dense distribution of Rayleigh clusters was derived from the concept of variance in local particle concentration. The fractal scattering regime for flocs larger than the ultrasound wavelength is further discussed. On the basis of the mean field approach proposed by one of the authors of this article (Snabre and Mills, 1996) for the equilibrium size of reversible flocs in concentrated suspensions, we propose a rheo-acoustical model in the Rayleigh scattering regime to describe the shear stress dependence of the low-frequency backscattered power per unit of volume. This model only involves physical parameters such as particle adhesive energy and cluster deformability.

In the second section, flow-dependent changes in the low-frequency scattered power in concentrated suspensions were carried out in a plane-plane flow geometry device for hardened or deformable red cell aggregates in neutral dextran polymer solution. The effects of the particle volume fraction, particle deformability, and shear rate dependence on the ultrasound scattering power from a dense suspension of red cell clusters were investigated. The results of the rheo-acoustical experiments were examined within the framework of the effective medium approximation, and the ability of ultrasound scattering to give quantitative information on particle adhesiveness is further analyzed. Lastly, from the disaggregation shear stresses of the flowing suspension determined from rheo-acoustical experiments and from the microrheological model based on the fractal approach (Snabre and Mills, 1996), we describe the shear-thinning behavior of weakly aggregated, hardened, or deformable red cells.

ULTRASOUND SCATTERING THEORY

In this section, we consider weakly scattering particles or aggregates with acoustic properties close to those of the surrounding medium, and of size smaller than the ultrasound wavelength λ, which enables us to apply the Rayleigh ultrasound scattering theory. Consequently, the attenuation of the incident ultrasound wave due to viscous losses remains negligible, and the ultrasound scattering process mainly arises from the different modes of vibration (radial pulsations, or back and forth oscillations) in relation to either the compressibility or the density mismatches of the mechanical properties of continuous and particle phases (Rayleigh, 1945). Theoretical models of ultrasound scattering are based either on the continuum approach (Angelson, 1980; Mo and Cobbold, 1992) or the particle approach (Twersky, 1987; Mo and Cobbold, 1993; Bascom and Cobbold, 1995). The fundamental difference between these two approaches lies in the manner in which the random medium is modeled. In each case, the linearized wave equation solved by the Green's function approach led to an integral expression of the scattered waves in terms of density and compressibility changes. The continuum approach indeed recognizes that particles separated by less than $\lambda/2$ cannot be resolved by the transducer, and that the suspension can therefore be modeled as a continuum medium in which local fluctuations in density and compressibility give rise to the scattered waves (Angelson, 1980). In contrast, the particle approach tracks the position of every particle in the insonified region and sums the wavelets scattered from individual particles (Mo and Cobbold, 1993; Bascom and Cobbold, 1995). Recently, Mo and Cobbold (1992) introduced a new hybrid approach that sums the wavelets from elemental volumes or voxels $\approx \lambda/2\pi$ in size, i.e., small

enough for the incident wave to arrive with the same phase at every particle located within it. In the low-frequency scattering regime (Rayleigh scattering), the hybrid approach predicts that nearly isotropic scattered power scales as the variance of the particle number in a voxel. In contrast, for clusters larger than a voxel, isotropic Rayleigh scattering is no longer valid, and the scattered power becomes strongly anisotropic because of the angle-dependent destructive interference (Snabre et al., 2000).

Random distribution of weak uncorrelated scatterers

For a random distribution of uncorrelated particles in space, in the single scattering regime, each particle scatters the incident wave unaffected by the presence of other particles. The incoherent scattered intensity from a weakly scattering suspension is given by the algebraic addition of the intensity scattered by individual particles (Twersky, 1962, 1978, 1987). The low-frequency scattering coefficient $\chi(\mathbf{k},\mathbf{s})$, defined as the power scattered per unit solid angle from a unit volume, and for an incident plane wave of unit amplitude, then scales as the inverse of the scattering mean free path l

$$\chi(\mathbf{k},\mathbf{s}) \approx \frac{1}{l} \text{ with } l = \frac{1}{n\sigma(\mathbf{k},\mathbf{s})}, \tag{1}$$

where n is the average number of scatterers per unit of volume, and $\sigma(\mathbf{k},\mathbf{s})$ is the differential scattering cross-sectional area of a weak scatterer with a volume V and an arbitrary shape that is given by the Green's function approach (Rayleigh, 1872)

$$\sigma(\mathbf{k},\mathbf{s}) = \pi^2\nu^4V^2(\kappa_o\rho_o)^2\times\left[\left(\frac{\kappa_p-\kappa_o}{\kappa_o}\right)+\left(\frac{\rho_p-\rho_o}{\rho_p}\right)\frac{\mathbf{k},\mathbf{s}}{ks}\right]^2, \tag{2}$$

where $\mathbf{k}$ and $\mathbf{s}$ are, respectively, the incident and scattered wave number vectors, ν is the ultrasound frequency, κ_p, κ_o, and ρ_p, ρ_o are the compressibilities and densities of the scatterers and suspending medium, and $c_o = 2\pi\nu/k = (\kappa_o\rho_o)^{-1/2}$ is the phase velocity in the suspending medium. In the Rayleigh scattering regime, the scattered power is proportional to the square of the particle volume and further scales as the fourth power of the ultrasound frequency ν. For human red cells suspended in saline solutions, the fourth-order frequency dependence was well confirmed (Shung et al., 1976).

Random distribution of weak correlated scatterers

Departure from independent scattering occurs in densely packed systems where the scatterers can no longer be treated as independent, because the proximity effects in highly concentrated suspensions, and hence the correlation effects, lower the ultrasonic scattered power, on account of the destructive interference of the wavelets arising from a dense distribution of scatterers (Twersky, 1962; Yuan and Shung, 1988).

In the Rayleigh scattering regime, coherent addition of the scattered waves leads to the ultrasound scattering coefficient $\chi(\mathbf{k},\mathbf{s})$, defined from the scattering mean free path l as

$$\chi(\mathbf{k},\mathbf{s}) = \frac{1}{l} \text{ with } l = \frac{1}{n\sigma(\mathbf{k},\mathbf{s})W(\mathbf{k},\mathbf{s})}, \tag{3}$$

where $W(\mathbf{k},\mathbf{s})$ is the packing factor derived from the Percus-Yevick pair correlation, which accounts for dependent scattering in dense systems (Twersky, 1978, 1987). However, the packing factor viewpoint involves complex statistical mechanics and provides unclear physical insight. In fact, the packing factor derived from the Percus-Yevick approximation only involves the particle volume fraction with no dependence upon the flow conditions, and remains empirical (Mo and Cobbold, 1993).

One may thus consider the concept of variance in local particle volume fraction derived from the hybrid approach (Mo and Cobbold, 1992) that sums the wavelets from elemental voxels $\approx \lambda/2\pi$ in size small enough for the incident wave to arrive with the same phase at every particle located within it. The scattered power can be split into one part that arises from a crystalline phase that gives no net contribution because of destructive wave interference, and another part representing contributions from independent fluctuations in the particle number ω within elemental voxels with a volume ΔV and size $\approx \lambda/2\pi$. The low-frequency scattered power from a dense suspension therefore scales as the variance $\overline{\text{var}(\omega)} = \overline{\omega^2} - \overline{\omega}^2$ of the particle number ω, averaged over the insonified region (Mo and Cobbold, 1992, 1993). Thus,

$$\chi(\mathbf{k},\mathbf{s}) = \frac{1}{l} \text{ with } l = \frac{1}{n\sigma(\mathbf{k},\mathbf{s})(\overline{\text{var}(\omega)}/\overline{\omega})}, \tag{4}$$

and $n = \overline{\omega}/\Delta V$.

Alternatively, the space average variance $\overline{\text{var}(\omega)} = \overline{\omega}W(\phi) = \Delta V\phi W(\phi)/V$ of particles in a voxel can be defined as a function of the packing factor $W(\phi)$ that unifies Eqs. 3 and 4.

Reversible fractal clusters

Within the framework of fractal aggregation and for a homogeneous flocculation process, ultrasonic scattering from a Rayleigh cluster is coherent, and the scattering cross-sectional area $\sigma_a(\mathbf{k},\mathbf{s})$ of a cluster of arbitrary shape is proportional to the square of the particle number N in the fractal cluster

$$\sigma_a(k,s) = N^2\sigma(\mathbf{k},\mathbf{s}) \text{ for } kaN^{1/D} \ll 1, \tag{5}$$

where D is the fractal dimension of aggregates.

According to the hybrid approach model for correlated Rayleigh aggregates, the directional scattering coefficient $\chi_a(\mathbf{k},\mathbf{s})$ from a dense distribution of Rayleigh clusters is therefore given by

$$\chi_a(\mathbf{k},\mathbf{s}) \approx \frac{1}{l_a} \text{ with } l_a \approx \frac{1}{n_a\overline{\sigma_a(\mathbf{k},\mathbf{s})}(\overline{\text{var}_a(\omega)}/\overline{\omega})}, \quad (6)$$

where $\overline{\text{var}_a(\omega)}$ is the average variance of the particle number ω in a voxel, $n_a = n/\overline{N}$, the average number of clusters per unit volume, and $\overline{N}$, the mean particle number in a fractal cluster.

Cluster growth increases the variance in particle number, because each voxel can gain or lose a large number of elementary particles. At a first approximation, the variance $\overline{\text{var}_a(\omega)}$ increases linearly with the volume fraction ϕ_a of the aggregates, and can be reasonably approximated by the scaling relationship:

$$\overline{\text{var}_a(\omega)} = \frac{\phi_a}{\phi}\overline{\text{var}(\omega)} \text{ for } N \ll (ka)^{-D}. \quad (7)$$

Substituting for the average variance in Eqs. 5 and 6 then gives:

$$\chi_a \approx \frac{1}{l_a} \text{ with } l_a = \frac{1}{n_a\overline{N^2}(\phi_a/\phi)\sigma(\mathbf{k},\mathbf{s})(\overline{\text{var}(\omega)}/\omega)}. \quad (8)$$

We further define the normalized ultrasonic scattering coefficient $\chi_r = \chi_a(\mathbf{k},\mathbf{s})/\chi(\mathbf{k},\mathbf{s}) \approx l/l_a$. Using Eqs. 3 and 8, the dimensionless ultrasonic scattering coefficient χ_r in the Rayleigh regime then becomes

$$\chi_r(k,s) = \frac{\chi_a(\mathbf{k},\mathbf{s})}{\chi(\mathbf{k},\mathbf{s})} \approx \frac{l}{l_a} = \frac{n_a}{\overline{n}}\frac{\phi_a}{\phi}\overline{N^2} = \frac{\overline{N^2}}{\overline{N}}\frac{\phi_a}{\phi}, \quad (9)$$

where $\phi_a/\phi = (n_a\overline{V}_a)/(nV) = \overline{V_a}/(\overline{N}V)$ and $\overline{V_a}$ is the average volume of the clusters. For a weak standard deviation of the cluster size distribution ($\overline{N^2} \approx \overline{N}^2$), the ultrasonic scattering power is nearly isotropic in the Rayleigh regime, and scales as the average volume $\overline{V}_a$ of clusters

$$\chi_r \approx \frac{\overline{V_a}}{V} \approx \left(\frac{R}{a}\right)^3 \text{ for } N \ll (ka)^{-D}, \quad (10)$$

where R is the mean radius of the aggregates.

Far field coherence effects determine the cluster volume dependence of the scattering coefficient χ_r that would scale as $(n_a/n)(\sigma_a/\sigma) \approx N \approx R^D$ when neglecting the variance term in Eqs. 4 and 6. One can indeed expect the fractal dimension of clusters not to affect the dimensionless ultrasonic scattering coefficient χ_r because the transducer cannot resolve the internal structure of aggregates smaller than voxels. Consequently, the dimensionless ultrasonic scattering coefficient χ_r can be interpreted as an aggregation index in the Rayleigh scattering regime ($kR \ll 1$).

Fractal scattering regime

For clusters larger than a voxel ($kR \gg 1$), the hybrid approach is no longer valid, and ultrasound scattering becomes strongly anisotropic because of angle-dependent destructive interferences. When considering the scattering wave number $\mathbf{q} = \mathbf{s}-\mathbf{k}$, the choice of a scattering angle θ sets a length scale $1/q = [2k\sin(\theta/2)]^{-1}$ under which scattering remains coherent (Lin et al., 1990). Therefore, one may decompose a cluster into smaller subunits of size $1/q$ with an average number $N_b \approx (q\,a)^{-D}$ of elementary particles. One subunit coherently scatters a power scaling as N_b^2. By contrast, the scattered waves from different subunits add incoherently, and the differential scattering cross-sectional area $\sigma_a(\mathbf{k},\mathbf{s})$ of an arbitrary shape cluster scales as the average number N/N_b of subunits in the aggregates. Thus,

$$\sigma_a(k,s) \approx \frac{N}{N_b}N_b^2\,\sigma(\mathbf{k},\mathbf{s}) \approx N^2\,Q(q\,R)\sigma(k,s), \quad (11)$$

where $Q(qR) \approx N_b/N \approx (qR)^{-D}$ is commonly referred as the structure factor in coherent optics (Lin et al., 1990) and describes the spatial correlations between particles in fractal structures. The fourth-order frequency law characterizing the Rayleigh scattering regime no longer applies for clusters larger than a voxel ($\sigma_a \approx a^6\,R^{-D}\,\lambda^{D-4}$). The crossover from the small-q scattering regime to the fractal scattering regime is much broader, and a more accurate expression of the structure factor $Q(qR)$ was proposed by Fisher and Burford (1967).

In the case of large clusters ($q\,R \gg 1$), the directional scattering cross section $\chi_a(\mathbf{k},\mathbf{s}) = n_a\,\sigma_a(\mathbf{k},\mathbf{s})$ per unit volume mainly depends on the scattering angle θ and the fractal dimension D of the clusters, and

$$\chi_a(\mathbf{k},\mathbf{s}) \approx \frac{\phi}{V}(q\,a)^{-D}\sigma(\mathbf{k},\mathbf{s}). \quad (12)$$

In the fractal scattering regime ($k\,R \gg \mathbf{1}$), the dimensionless ultrasonic scattering coefficient $\chi_r = \chi_a/\chi \approx (qa)^{-D}/W(\phi)$ is insensitive to cluster size and can no longer characterize the extent of particle aggregation.

REVERSIBLE FRACTAL CLUSTERS IN A SHEAR FLOW

Equilibrium size of flocs

Above a critical yield stress, the shear thinning behavior of weakly aggregated suspensions results from the rupture of the spanning network and finite clusters when the shear stress is increased (Potanin and Uriev, 1991; Wessel and

Ball, 1992; Snabre and Mills, 1996). Reversible clusters can grow in a shear field until they reach a maximum stable size R corresponding to a dynamic equilibrium between the formation and shear break-up of the aggregates. As shown by experimental investigations (Sonntag and Russel, 1987; Torres et al., 1991) and computer simulations (Potanin, 1993) the shear stress dependence of the equilibrium radius $R(\tau)$ of an isolated fractal cluster obeys the power law

$$\frac{R(\tau)}{a} \approx \left(\frac{\tau^*}{\tau}\right)^{\mathrm{m}} \text{ with } 1/3 \le m \le 1/2, \qquad (13)$$

where the critical shear stress $\tau^* \approx \Gamma/a$ for cluster break-up is related to the surface adhesive energy Γ(adhesive energy per unit contact area) and to the characteristic radius a of elementary particles. The break-up criterion $R^3(\tau) \approx CK\,a^2/\tau$ (Potanin, 1993) involves an unknown fragility parameter C and the spring constant K of the bonds between the particles. The fragility of the bonds depends on the reversibility of cluster deformation under the action of external stresses. Soft and rigid clusters represent the extremes of possible aggregate behavior (Snabre and Mills, 1996). Rigid clusters are more likely broken into secondary aggregates of approximately equal parts (''large-scale fragmentation'') because elastic deformations are transmitted over the whole structure (Snabre and Mills, 1996). On the other hand, soft structures are irreversibly deformed by external stresses and splits of individual particles and small clusters one-by-one until the cluster reaches a stable size (''surface erosion'') (Snabre and Mills, 1996).

One may consider in the following, a mean field theory proposed by one of the authors of this article (Snabre and Mills, 1996) giving a scaling law similar to the phenomenological Eq. 13, with $m = 1/3$ for rigid clusters and $m = 1/2$ for deformable aggregates, in agreement with experimental investigations (Torres et al., 1991; Sonntag and Russel, 1987) and computer simulations (Potanin, 1993).

Rheo-acoustical model

In this section, we propose a rheo-acoustical model to describe the shear stress dependence of the ultrasound cross-sectional area per unit of volume, in relation to the physical parameters of particle adhesiveness and cluster deformability. When both the cluster volume dependence of the volumetric scattering power and the break-up criterion are taken into account, the ultrasound backscattered coefficient $\chi_{\mathrm{r}}(\tau)$ from a dense suspension of reversible aggregates, in the Rayleigh scattering regime ($kR \ll 1$) obeys the following power law

$$\chi_{\mathrm{r}}(\tau) = \left(\frac{R(\tau)}{a}\right)^3 \approx 1 + \left(\frac{\tau^*}{\tau}\right)^{3\mathrm{m}} \text{ with } 1/3 \le m \le 1/2, \quad (14)$$

and $\tau^* \approx \Gamma/a$,

where particle adhesiveness and cluster deformability, respectively, determine the critical shear stress τ^* for cluster break-up and the exponent m. Neither the particle volume fraction within the aggregates nor the fractal dimensionality affect the size of Rayleigh clusters or the scattering behavior. In contrast, the internal structure of the aggregates and the amount of fluid trapped within them determine both the suspension viscosity and the average shear stress τ experienced by interacting clusters (Snabre and Mills, 1996).

RHEO-ACOUSTICAL EXPERIMENTS

We explored the effects of particle volume fraction and shear rate dependence on the low-frequency scattering power from a dense suspension of hardened or deformable red cell aggregates and further examined the self-consistent field approximation used in the microrheological model proposed by one of the authors (Snabre and Mills, 1996). Rheo-acoustical experiments were carried out in a plane-plane flow geometry device. An 8-MHz piezoelectric transducer was used to emit acoustic bursts and detect the backscattered waves from red cell clusters. Red cells of mean radius ≈ 2.8 μm (mean volume $V = 87\ \mu\mathrm{m}^3$) can be considered as weak Rayleigh scatterers when probed with an 8-MHz ultrasound wave of wavelength ≈ 200 μm, because of the likeness of the acoustic properties (i.e., the density and compressibility) of red cells and of saline solution (Shung et al., 1976). Considering the acoustical properties of the erythrocytes such as density $\rho_{\mathrm{p}} \approx 1092\ \mathrm{kg/m^3}$ and compressibility $\kappa_p \approx 34.1 \times 10^{-11}\ \mathrm{m^2/N}$ and those of the physiological saline solution ($\rho_{\mathrm{o}} \approx 1005\ \mathrm{kg/m^3}$, $\kappa_{\mathrm{o}} \approx 44.3 \times 10^{-11}\ \mathrm{m^2/N}$), the Rayleigh formula (Eq. 2) predicts a backscattering cross-sectional area $\sigma(\mathbf{k}, -\mathbf{k}) \approx 6 \times 10^{-14}\ \mathrm{cm^2}$ for a single red cell in saline solution.

Properties of red cell aggregates

Normal red cells or erythrocytes are biconcave disks of 8-μm mean diameter and 2-μm thickness when suspended in an isotonic phosphate buffered saline solution (PBS) (osmolarity 300 mOsmol; ionic strength 150 mM; and pH = 7.4). Blood was obtained from healthy human donors and used on the day of withdrawal. After centrifugation and removal of the plasma and white cell-platelet layer, red blood cells were washed twice in PBS (10 min at 3000 rpm).

Cross-linking of the skeleton proteins in a glutaraldehyde solution produces hardened red cells. The glutaraldehyde treatment does not affect red cell electrophoretic mobility and thus hardly alters the outer surface of the cell (Snabre et al., 1985). Glutaraldehyde-fixed red cells were prepared by suspending 1 vol of washed cells in 10 vol of 2% glutaraldehyde saline solution for 60 min at room temperature. Hardened red cells were then washed twice in PBS. Lastly, normal or hardened red cells were suspended in dextran saline solutions (ionic strength, 150 mM).

Above a molecular weight of $\sim 4 \times 10^4$ dalton, dextran polymer induces reversible aggregation of human red cells (Snabre et al., 1985; Chien and Jan, 1975). The extent of red cell aggregation increases with dextran molecular weight and polymer concentration, but the suspension stability is recovered at high dextran concentrations $\varphi > 3 - 5\,\mathrm{g}\%$. Reversible red cell flocculation is usually attributed to macromolecular bridging between cell surfaces (Chien and Jan, 1975). However, the nature of red cell interaction in polymer solution remains controversial up to now. There is indeed good evidence that in dextran solutions red cell aggregation results from polymer depletion, as at high polymer concentrations, the disaggregation stage arises from the penetration of chains within the cell surface coat (Snabre, 1988; Neu and Meiselman, 2002).

The fractal dimension of two-dimensional normal or hardened red cell aggregates was determined by one of the authors (Snabre and Mills, 1996) from the visualization under microscope of clusters between two glass plates after previous dispersion of the suspension. The particle number dependence of the cluster size yielded the fractal dimensions $D = 1.59 \pm 0.03$ and $D = 1.56 \pm 0.04$, respectively, for normal and hardened red cells, respectively, in 3 g% dextran 80-PBS (Snabre and Mills, 1996) in good agreement with the predictions of the Reaction Limited Aggregation model ($D \approx 1.55$ for $d = 2$) representative of reversible flocculation.

Ultrasonic experimental setup

For the ultrasonic experimental device, we used an Altuglas (Altulor, Paris, France) cylinder (diameter 94 mm) divided into two compartments by an Altuglas plate perpendicular to the vertical axis of a plane-plane flow device (Fig. 1). The flow field was generated in the upper compartment between the stationary plate and an upper rotating Altuglas plane disk driven by a stepper motor. In the lower compartment, which

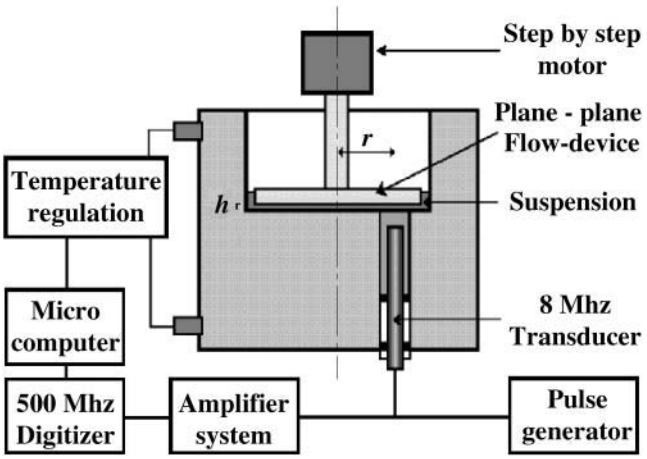

FIGURE 1 Schematic representation of the ultrasonic technique to investigate the ultrasound backscattering from a flocculated red cell suspension in a plane-plane flow device.

was filled with water to ensure good ultrasonic coupling, a transmitter receiver circular transducer (Vermon, Tours, France) (incident beam diameter $d \approx 5\,\mathrm{mm}$) was driven by a pulse function generator that emits electrical sinusoidal pulses at a frequency of 8 MHz (resonant frequency of the transducer) and a repetition rate of 200 Hz. The piezoelectric nonfocused transducer connected to the Altuglas plate by an acoustic window emits short ultrasonic bursts (pulsewidth $\delta t = 0.4\,\mu\mathrm{s}$) in the direction perpendicular to the plane-plane flow device. The pulsewidth is short enough to enable the scattering from the suspension to be separated from the specular reflections of the plates (axial resolution $\delta z = \delta t\, c_\mathrm{s}/2 \approx 0.3\,\mathrm{mm}$ where $c_\mathrm{s} \approx 1570\,\mathrm{m/s}$ is the sound velocity in the suspension). The distance $z \approx 41$ mm from the piezoelectric ceramic to the insonified volume between the plates was chosen so as to be in the far field of the transducer (the transition point from the near field zone to the far field zone is located at the distance $z_\mathrm{o} \approx d^2/4\lambda \approx 32\,\mathrm{mm}$). The far field pattern of the transducer has a 5°-wide central lobe so that the lateral resolution δx is of the order of 5 mm.

The water temperature in the lower compartment was maintained at 25°C and controlled with ±0.5°C accuracy. The average distance $r = 30$ mm from the axis of the plane-plane flow device and the angular velocity of the rotating disk ($8\times10^{-5}\,\mathrm{rds}^{-1} < \omega < 80\,\mathrm{rds}^{-1}$) determined the average local shear rate $\gamma \approx r\omega/h$ in the insonified region across the gap width h ($10^{-3}\,\mathrm{s}^{-1} < \gamma < 10^3\,\mathrm{s}^{-1}$ for $h = 2.5$ mm). The echo either reflected from the wall surfaces or scattered from the suspension was detected by the same transducer. The radio frequency signal delivered by the transducer was first amplified and filtered before direct sampling using a Tektronix 520 digitizer (Beaverton, OR). The digitized signals were downloaded onto a microcomputer (Macintosh Centris 650, Cupertino, CA) where gating and power calculations are performed. Time gating of the digitized signal provides a way of measuring the RMS powers P_r and P_s of the echo corresponding either to specular reflections at wall/suspension interfaces (considered as a reference acoustic reflector) or to scattering from a specified volume between the plates. The backscattering coefficient $\chi(\mathbf{k}, -\mathbf{k})$ is derived from the relation (Sigelmann and Reid, 1973; Hanss and Boynard, 1979)

$$\chi(\mathbf{k}, -\mathbf{k}) = \left(\frac{\rho_\mathrm{w} c_\mathrm{w} - \rho_\mathrm{s} c_\mathrm{s}}{\rho_\mathrm{w} c_\mathrm{w} + \rho_\mathrm{s} c_\mathrm{s}}\right)^2 \frac{z^2}{A\delta z}\frac{P_\mathrm{s}}{P_\mathrm{r}}, \qquad (15)$$

where ρ_w and ρ_s are, respectively, the densities of the Altuglas wall and the suspension, c_w and c_s the sound velocities in the same two previous media, z the distance between the front face of the transducer and the insonified region, A the cross-sectional area of the ultrasound beam, and $\delta z = \delta t\, c_\mathrm{s}/2$ the axial resolution of the transducer.

The shear viscosity of the suspensions was measured at 25°C in a couette viscometer (RCHAIX-MCCA, Paris, France) and calculated with ±3% accuracy from the steady-

state torque reading. Before each measurement, the sample was sheared at a high shear rate, to avoid both sedimentation and memory effects due to shear-induced restructuration processes.

Shear break-up of hardened or deformable red cell aggregates

We measured the ultrasonic backscattered power from normal red cells suspended in dextran 70-PBS solution for shear rates in the range of $0.1\,s^{-1} < \gamma < 50\,s^{-1}$. The suspension was first dispersed in an intense flow ($\gamma = 128\,s^{-1}$) before the relevant shear rate γ was imposed at time $t = 0$ (Fig. 2). Particle flocculation resulted in an increase in the ultrasound backscattered power, which reached a stationary level after ~2 min. The flow was quickly stopped to suppress any orientation of deformable particles and anisotropy of the suspension microstructure. After the flow had stopped, the ultrasonic backscattering coefficient χ_a was representative of the dynamic aggregation equilibrium for random particle orientation (Fig. 2). No time-dependent restructuration processes or significant memory effects were observed for hardened red cell aggregates in the low shear regime (Fig. 2). Aggregated rigid particles only establish contact points during the adhesion process, and the low internal variation energy of the suspension associated with particle aggregation then prevents any shear-induced restructuration process (Snabre and Mills, 1996). In contrast,

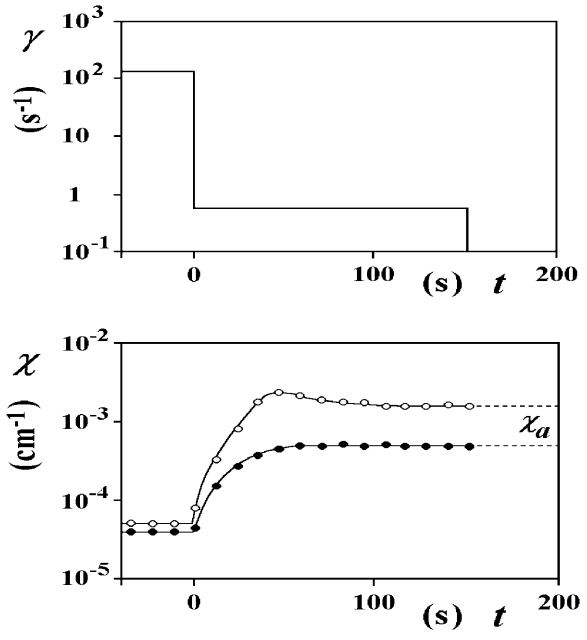

FIGURE 2 Time dependence of ultrasonic backscattering coefficient $\chi(t)$ for normal (○) and hardened (●) red blood cells in 3 g% dextran 70-PBS from the flow setting ($\gamma = 0.6\ s^{-1}$ for $t > 0$) and the establishment of a dynamical equilibrium to flow stoppage ($\phi = 0.15$, $T = 25°C$, and $I = 150$ mM). The suspension was previously dispersed in an intense flow ($\gamma = 128\ s^{-1}$ for $t < 0$) before imposing the relevant shear rate $\gamma = 0.6\ s^{-1}$.

an increased backscattering coefficient and shear-induced restructuration of the infinite network for deformable red cell clusters subjected to low shear rates was observed as shown in Fig. 2. Such a restructuration process preferentially occurs for strongly aggregated deformable particles (Fig. 3) and mainly results in memory effects in the rheology of aggregated suspensions (Snabre and Mills, 1996; Snabre, 1988).

Fig. 4 shows the shear rate dependence of the ultrasonic backscattering coefficient $\chi_a(\gamma)$ upon the particle volume fraction, for deformable red cells suspended in 3 g% dextran 70-PBS ($0.16 \le \phi \le 0.35$). When both the particle volume fraction and the shear rate γ are increased, the steady ultrasonic backscattering coefficient $\chi_a(\gamma)$ decreases because of the increase in spatial correlation among the Rayleigh clusters that induces destructive interference of the far field scattered waves and the shear break-up of red cell clusters into smaller ones. At higher shear rates of $\gamma > 20\,s^{-1}$, clusters are broken up into individual particles and the ultrasonic backscattering coefficient is close to $\chi \approx 5 \times 10^{-5}\ cm^{-1}$, which is higher than the predictions based on the Percus-Yevick approximation ($\chi(\mathbf{k},-\mathbf{k}) = \phi\sigma(\mathbf{k},-\mathbf{k})W(\phi)/V \approx 3 \times 10^{-5}\ cm^{-1}$ with $V \approx 87\ \mu m^3$, $\sigma(\mathbf{k},-\mathbf{k}) \approx 6 \times 10^{-14}\ cm^2$ and $W(\phi) = (1-\phi)^4/(1+2\phi)^2$) (Snabre et al., 2000). The variance in the number of particles in a voxel scales as $\phi\ W(\phi)$ and indeed displays limited variations over the range $0.16 \le \phi \le 0.35$. Flow disturbances and turbulence effects may increase local fluctuations in the particle concentration. The deformation orientation of deformable red cells at higher shear rates further enhances the ultrasonic backscattering coefficient. However, no shear dependence was observed below $200\,s^{-1}$ for the ultrasound scattered power from nonaggregated red cell suspensions, in agreement with recent reports (Van Der Heiden et al., 1995).

Now, we consider the dimensionless backscattering coefficient $\chi_r = \chi_a/\chi$ for hardened red cell suspensions (Fig. 5 *a*) or deformable red cell suspensions (Fig. 5 *b*), and

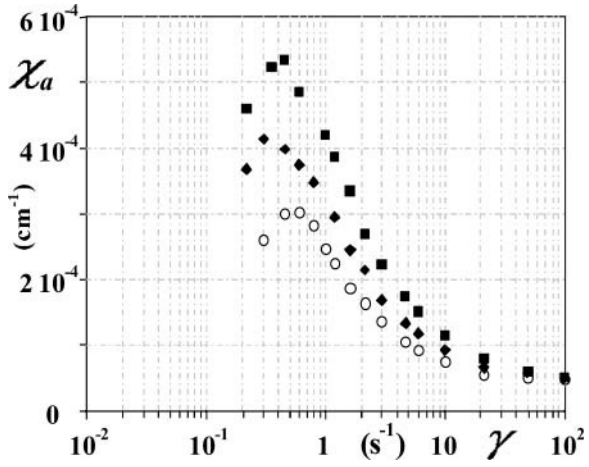

FIGURE 3 Ultrasonic backscattering coefficient χ_a versus shear rate for deformable red cells in 3 g% dextran 70-PBS (○), 3 g% dextran 170-PBS (♦), and 3 g% dextran 500-PBS (■). Particle volume fraction $\phi = 0.30$.

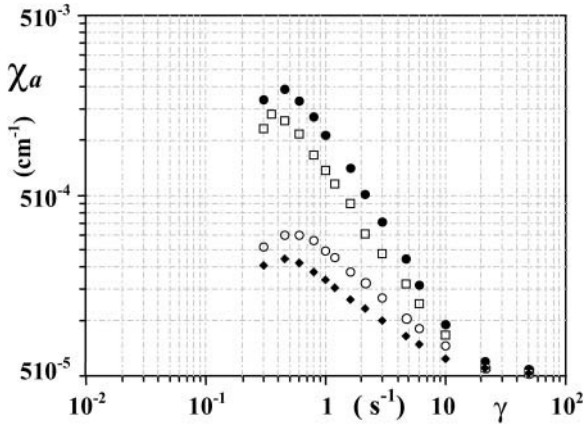

FIGURE 4 Ultrasonic backscattering coefficient χ_a versus shear rate γ for deformable red cells in 3 g% dextran 70-PBS. Particle volume fraction $\phi = 0.16$ (●), $\phi = 0.20$ (□), $\phi = 0.30$ (○), and $\phi = 0.35$ (♦).

define the critical shear rate γ_c in term of the extrapolated intercept (Snabre and Mills, 1996; Snabre, et al., 1987, 2000). Under well-defined shear rate conditions, particle crowding or rigidity increases the viscosity of the suspension and improves the dissociation efficiency of the flow, resulting in a lower normalized backscattering coefficient χ_r. Raising the particle volume fraction therefore shifts the critical shear rate $\gamma_c(\phi)$ for cell disaggregation toward lower values (Table 1 or 2).

We further report the dimensionless backscattering coefficient χ_r against the shear stress $\tau = \mu_a(\gamma)\gamma$ for both hardened and normal red cells suspended in dextran saline solution to account for the microrheological conditions around the clusters whatever the particle volume fraction or cell deformability (Fig. 6, *a* and *b*). In accordance with the self-consistent field model (Snabre and Mills, 1996; Snabre et al., 1987, 2000), the dimensionless backscattering coefficient χ_r versus the shear stress $\tau = \mu_a(\gamma)\gamma$ displays no significant dependence on particle volume fraction or cell deformability, because the local shear stress determines the equilibrium size of interacting flocs in a dense suspension. The master curves $\chi_r(\tau)$ (Fig. 6, *a* and *b*) thus well establish the validity of the effective medium approximation used in the microrheological models (Snabre and Mills, 1996; Snabre et al., 1987) and further indicate that coherence effects among scatterers only involve the average particle volume fraction, because the transducer cannot resolve the structure of aggregates smaller than a voxel (Snabre et al., 2000).

The experimental critical disaggregation shear stress for rigid red cells $\tau_c \approx 0.45\mathrm{N/m^2}$ (Fig. 6 *a*) or deformable red cells $\tau_c \approx 0.47\mathrm{N/m^2}$ (Fig. 6 *b*), defined in terms of the extrapolated intercept for near complete cell dispersion, is representative of cell adhesiveness and reflects the mechanical force required to disrupt adhesive bonds between two particles. According to the Derjaguin theory, the critical force $F_c \approx \tau_c a^2$ required to break a doublet scales as Γa (Γ is the surface adhesive energy). Taking $a \approx 4$ μm,

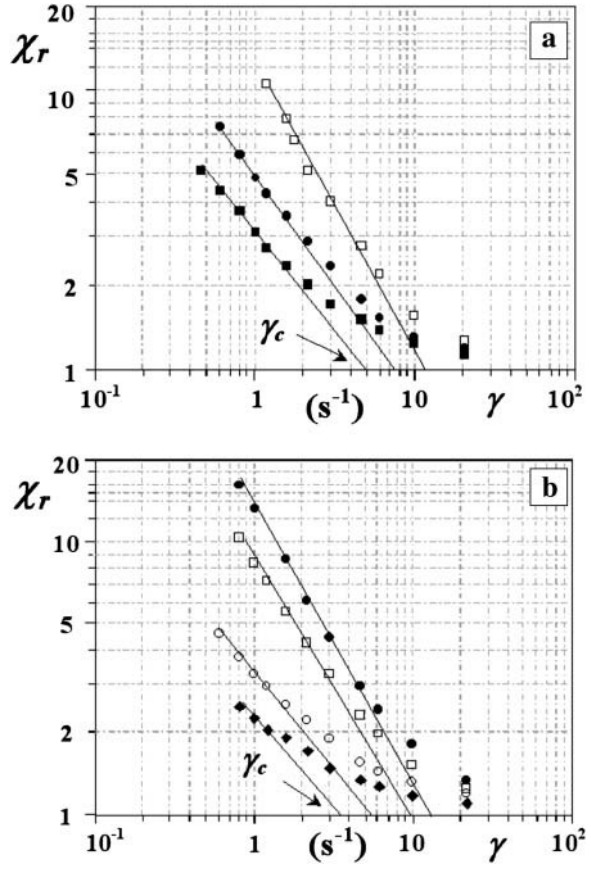

FIGURE 5 Dimensionless ultrasonic backscattering coefficient χ_r versus shear rate γ for hardened (*a*) or deformable (*b*) red cells in 3 g% dextran 70-PBS. Particle volume fraction (*a*) $\phi = 0.15$ (□), $\phi = 0.25$ (●), and $\phi = 0.30$ (■), (*b*) $\phi = 0.16$ (●), $\phi = 0.20$ (□), $\phi = 0.30$ (○), and $\phi = 0.35$ (♦),

we therefore derive a surface adhesive energy $\Gamma \approx \tau^* a \approx 1.8 \times 10^{-6}\,\mathrm{N/m}$, in good agreement with earlier estimations based either on rheo-optical experiments ($\Gamma \approx 2 \times 10^{-6}\,\mathrm{N/m}$ for red cells in 2 g% dextran 80) (Snabre and Mills, 1996; Snabre et al., 1987) or the equilibrium shape of deformable red cell doublets (Skalak et al., 1981). Glutaraldehyde treatment of red cells causes irreversible alterations of the endoface membrane proteins and reduces membrane deformability without significantly changing the surface adhesive energy (Snabre and Mills, 1996).

Deformable and rigid red cell clusters thus obey the same breaking-up behavior, in a simple shear flow, and can be

TABLE 1 Experimental values of disaggregation shear rate γ_c, relative shear viscosity $\mu_r(\gamma_c)$, and critical disaggregation shear stress $\tau_c = \mu_r(\gamma_c)\mu_o\gamma_c$ for hardened red cells suspended in 3 g% dextran 70-PBS (liquid viscosity $\mu_o = 1.82$ mPa×s)

ϕ	γ_c (s^{-1})	$\mu_r(\gamma_c)$	τ_c (N/m^2)
0.15	12.9	1.92	0.45
0.25	7.3	3.4	0.452
0.30	5	4.93	0.449

TABLE 2 Experimental values of disaggregation shear rate γ_c, relative shear viscosity $\mu_r(\gamma_c)$, and critical disaggregation shear stress $\tau_c=\mu_r(\gamma_c)\mu_o\gamma_c$ for deformable red cells suspended in 3 g% dextran 70-PBS (liquid viscosity $\mu_o=1.82$ mPa×s)

ϕ	γ_c (s^{-1})	$\mu_r(\gamma_c)$	τ_c (N/m^2)
0.16	14.5	1.79	0.472
0.20	9.2	2.81	0.470
0.30	5.4	4.84	0.475
0.35	3.3	7.9	0.474

considered as soft clusters undergoing irreversible deformation under the action of external shear stresses, because of weak bonding energy between particles. In the case of hardened red cells, clusters likely remain soft, because the biconcave shape of erythrocytes allowed the particles to roll at their contact point. For soft aggregates ($m = 1/2$) of fractal dimension $D = 2$, the dimensionless backscattering coefficient $\chi_r(\tau)$ may be estimated from Eq. 14:

$$\chi_r(\tau) = \left(\frac{R(\tau)}{\tau}\right)^3 \approx 1 + \left(\frac{\tau^*}{\tau}\right)^{3/2}. \qquad (16)$$

For the critical shear stresses $\tau^* = 0.25$ N/m^2 (Fig. 7 *a*) or $\tau^* = 0.28$ N/m^2 (Fig. 7 *b*), the above relation well describes the shear stress dependence of the dimensionless backscattering coefficient $\chi_r(\tau)$ in the Rayleigh scattering regime. For normal or rigid red cells in dextran 70-PBS, particle flocculation occurs above the critical dextran concentration $\varphi \approx 1.5$ g% (Fig. 8). As dextran is added, the critical disaggregation shear stress τ_c rises and then decreases for polymer concentrations higher than 4 g% (Fig. 8). The disaggregation behavior at high dextran polymer concentrations $\varphi > 6g\%$ is very sensitive to the structure of the outer polymeric coat (or glycocalyx) of biological membranes (Othmane et al., 1990).

Note, however, that this rheo-acoustical model is only valid as long as the clusters remain smaller than the voxels.

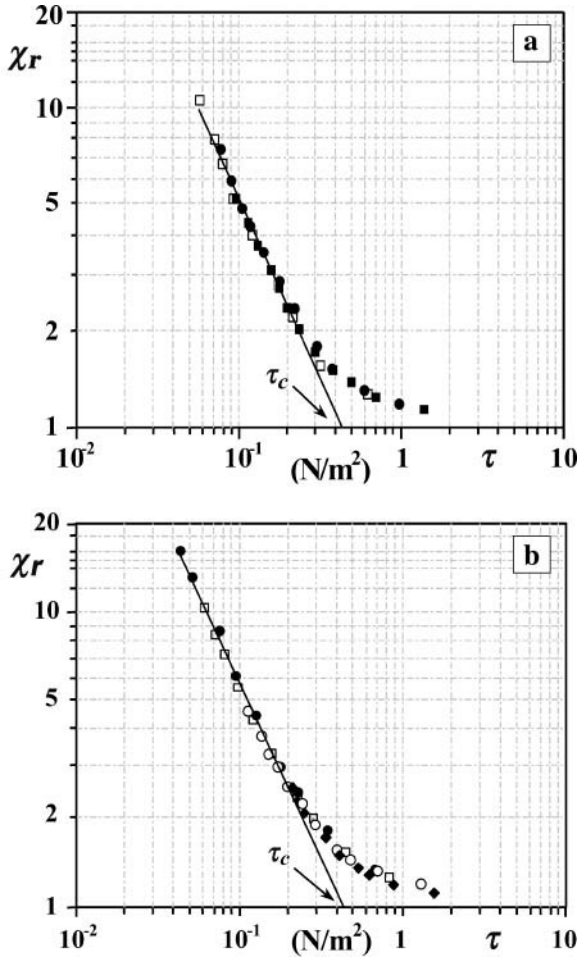

FIGURE 6 Dimensionless ultrasonic backscattering coefficient χ_r versus shear stress τ for hardened (*a*) or deformable (*b*) red cells suspended in 3 g% dextran 70-PBS. Particle volume fraction (*a*) $\phi = 0.15$ (□), $\phi = 0.25$ (●), and $\phi = 0.3$ (■), (*b*)$\phi = 0.16$ (●), $\phi = 0.20$ (□), $\phi = 0.30$ (○), and $\phi = 0.35$ (♦).

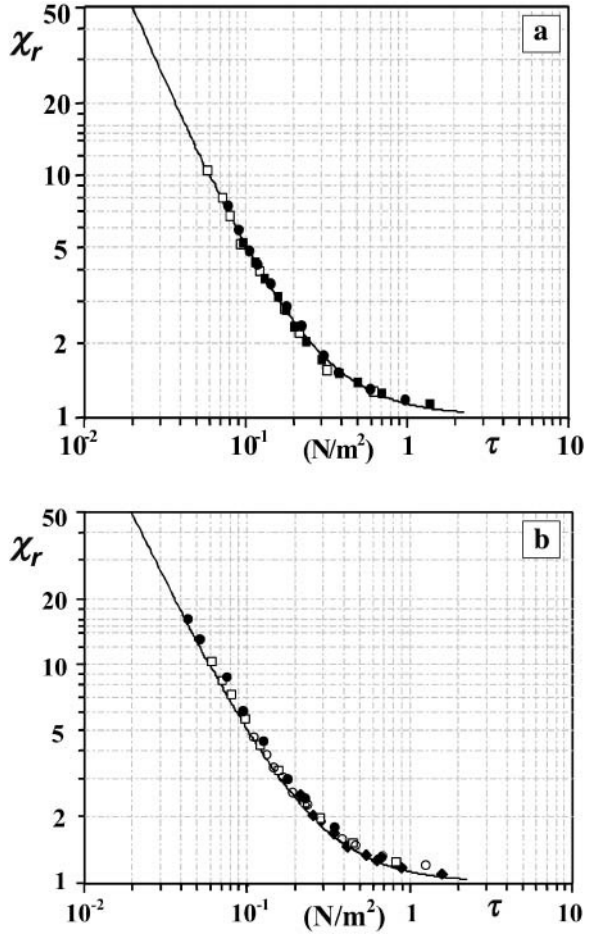

FIGURE 7 Dimensionless ultrasonic backscattering coefficient χ_r versus shear stress τ for hardened (*a*) or deformable (*b*) red cells suspended in 3 g% dextran 70-PBS. Particle volume fraction (*a*) $\phi = 0.15$ (□), $\phi = 0.25$ (●), and $\phi = 0.3$ (■), (*b*)$\phi = 0.16$ (●), $\phi = 0.20$ (□), $\phi = 0.30$ (○), and $\phi = 0.35$ (♦). The solid curves were calculated from Eq. 14 with $m = 1/2$ and $\tau^* = 0.25$ N/m^2 (*a*) or $\tau^* = 0.28$ N/m^2 (*b*). The rheo-acoustical model predicts a power law scaling as $(\tau^*/\tau)^{3m}$ with an exponent $m = 1/2$ for soft clusters.

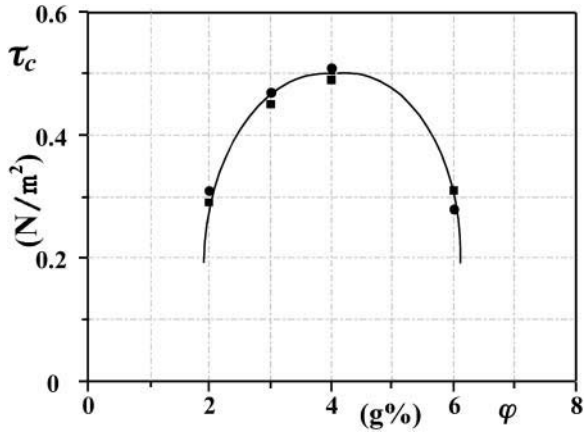

FIGURE 8 Critical disaggregation shear stresses τ_c determined by ultrasound scattering versus dextran 70 concentration for rigid (■, $\phi = 0.25$) or deformable red cells (●, $\phi = 0.30$).

Here, the maximum value $\chi_r \approx 30$ of the backscattering coefficient in the low shear regime corresponds to a mean cluster diameter of $2a\chi^{1/3} \approx 25\,\mu$m. This diameter is close to the characteristic size $\lambda/2\pi = 30\,\mu$m of the voxels when the suspension is probed with 8-MHz ultrasound waves (Fig. 6, *a* or *b*). Rayleigh scattering from blood is no longer valid at low shear rates $\gamma < 1\,s^{-1}$, especially for strong red cell aggregation and high ultrasound frequency ($kR = 2\pi\nu R/c_o$) (Yuan and Shung, 1988). The dimensionless scattering coefficient accounting for spatial correlations among clusters scales as $\chi_r = \chi_a/\chi \approx (qa)^{-D}/W(\phi)$ with $1/q = [2k\sin(\theta/2)]^{-1}$ (Snabre et al., 2000) and becomes sensitive to the scattering angle θ and fractal dimension D of structures ($kR \gg 1$) and with an ultrasound frequency dependence $\chi_r \approx \nu^{4-D}$ (Snabre et al., 2000; Haider et al., 2000). For most biological media with a long-range structure such as liver, the frequency dependence of the ultrasound scattered power obeys the power law $\chi_a \approx \nu^f$ with $f \approx 2$ (Dunn et al., 1969; Javanaud, 1989) indicating a fractal scattering regime and further giving a fractal dimension $D = 4 - f \approx 2$.

SHEAR VISCOSITY

Hardened red cell aggregates

We now consider the microrheological model using the self-consistent field approximation and introducing a Newtonian viscosity law $\mu(\phi, \phi^*)$ for hard spheres in purely hydrodynamic interactions (Mills, 1985; Snabre and Mills, 1996). Changes in the effective volume fraction or maximum packing fraction ϕ^* of the structural units determine the non-Newtonian behavior of the suspension. In the case of particle flocculation, fractal structures fill space and reach a maximum size $\hat{R}(\phi)$ above the gelation threshold ϕ_g as a consequence of cluster interpenetration. The infinite spanning network displays solid-like viscoelasticity behavior and roughly consists of a dense collection of fractal subclusters or ''blobs'' of size $\hat{R}(\phi) \approx a(\phi/\phi^*)^{1/D-3}$ packed with a volume fraction ϕ^* (Snabre and Mills, 1996). The shear break-up of these blobs determines the yield shear stress τ_o through the rupture criterion (Eq. 13) and the condition $R(\tau_o) = \hat{R}(\phi)$ (Snabre and Mills, 1996) so that:

$$\tau_o \approx \tau^* \left((\phi/\phi^*)^{\frac{1}{D-3}} - 1 \right)^{-\frac{1}{m}} \text{ for } \phi > \phi_g. \tag{17}$$

For a fractal dimension $D > 2$, clusters may be considered as impermeable, with strong hydrodynamic screening inside the aggregates. The shear viscosity $\mu_a(\phi_a, \phi^*)$ of a weakly aggregated suspension then follows from the reference rheological law $\mu(\phi, \phi^*)$ for hard spheres, from the effective volume fraction $\phi_a(\tau) \approx \phi(R/a)^{3-D}$ of clusters, and from the break-up criterion (Eq. 13). The effective medium approximation $\tau = \mu_a(\gamma)\gamma$ established from rheo-acoustical experiments (Snabre et al., 2000) gives a nonlinear expression of the shear viscosity. For soft clusters ($m = 1/2$) with a fractal dimension $D = 2$ and the reference law $\mu_a(\phi_a, \phi^*) = \mu_o(1-\phi)/(1-\phi/\phi^*)^2$ (Mills, 1985; Snabre and Mills, 1996), the microrheological model then leads to a Casson-like behavior (Snabre and Mills, 1996):

$$\sqrt{\tau} = \sqrt{\tau_o} + \sqrt{\mu\gamma}\left[1 - \frac{\phi}{1-\phi}\left(\frac{\tau^*}{\tau}\right)^{1/2}\right]^{1/2}, \tag{18}$$

with

$$\mu = \mu_o \frac{1-\phi}{(1-\phi/\phi^*)^2}. \tag{19}$$

Deformable red cell aggregates

In the case of deformable particles, cell orientation in shear flow and the formation of transient anisotropic structures with a higher maximum packing volume fraction ϕ^* enhance the non-Newtonian behavior. On the basis of the Kelvin-Voigt model and a linear expansion of the structure parameter $\phi^*(\gamma)$ in terms of the shear strain gradient in the flow's direction, a self-consistent approach then gives a nonlinear expression of the shear viscosity as a function of a Deborah number $\Omega = \gamma\vartheta_o$ (ϑ_o being the characteristic viscoelastic relaxation time of the structural units) (Snabre and Mills, 1996). Taking into account the nonlinear viscoelastic properties of red cell membranes, the shear viscosity of a dense suspension of deformable red cells is therefore given by Snabre and Mills (1996)

$$\mu(\phi,\gamma) = \frac{\mu_o(1-\phi)}{\left[1 - \frac{\phi}{\phi_o^*}\left(1 + \frac{\mu(\phi,\gamma)}{\mu_o}\frac{\beta(\mu_i/\mu_o)^{-1}(\vartheta_o\gamma)^{1/2}}{1+(\vartheta_o\gamma)^{1/2}}\right)^{-1}\right]^2}, \tag{20}$$

where ϕ_o^* is the maximum packing fraction around the zero shear rate limit, μ_i, the viscosity of the intracellular fluid ($\mu_i = 6\,\text{cP}$) and β, a constant. The variable $(\vartheta_o\gamma)^{1/2}$ arises from the specific viscoelastic nature of the red cell membrane, and appears in a phenomenological law often used to describe blood rheology (Quemada, 1978).

We determined the shear viscosity μ_a of hardened and deformable red cells suspended in 3 g% dextran 70-PBS when the particle volume fraction was varied $0.16 \le \phi \le 0.35$. The suspension was previously dispersed by shearing at 128 $s^{-1}$and then allowed to relax for 5 min. Steady-state shear experiments were performed by increasing the shear rate step-by-step and waiting for steady state before the measurements.

For soft clusters ($m = 1/2$) with a fractal dimension $D = 2$, Eqs. 18–20 describe the shear rate dependence of the relative viscosity for hardened red cell aggregates (Fig. 9, *top*) or deformable red cell aggregates (Fig. 9, *bottom*) fairly well. Aggregation phenomena dominate the rheological behavior in the low shear regime. By increasing the shear rate, clusters are progressively broken up and the relative shear viscosity decreases, because a lower fluid volume fraction is trapped inside the clusters. At high shear rates, deformable red cells become oriented and aligned in the flow, and the relative viscosity is then governed by the viscoelastic properties of the particles (Fig. 9, *bottom*). Critical disaggregation shear stresses τ^*, determined from rheo-ultrasonic and viscometry experiments, differ by a factor of 10 because particle flocculation dominates the rheological behavior in the low shear regime, and the shear viscosity is not very sensitive to the presence of small aggregates. No hysteresis phenomena arising from a shear-induced restructuration process were observed in the low shear regime for hardened red cell clusters (Fig. 9, *top*). Such a shear-induced restructuration process or the formation of a marginal layer free of particles near the viscometer walls may affect the rheology of red cell suspensions (Snabre and Mills, 1996; Snabre et al., 2000). As a restructuration process requires a significant increase in the internal energy of the aggregates and a large adhesive area between adjacent cell membranes (Snabre and Mills, 1996), cell deformability and adhesiveness strongly favor shear-induced restructuration of clusters, and contraction of the spanning network in the low shear regime (Snabre and Mills, 1996; Snabre, 1988). At low shear rates, the simultaneous appearance of a particle-free region near the viscometer walls therefore results in a decrease of the suspension viscosity (Snabre and Mills, 1996; Snabre, 1988). However, for moderate deformable red cell adhesiveness, shear-induced restructuration of clusters and the formation of a marginal layer by contraction of the spanning network remain negligible at low shear rates (Snabre and Mills, 1996; Snabre, 1988). Low shear viscosity measurements are only very sensitive to both the rheological history of the suspension and viscometer geometry only for a strong deformable red cells aggregation (Snabre and Mills, 1996; Snabre, 1988).

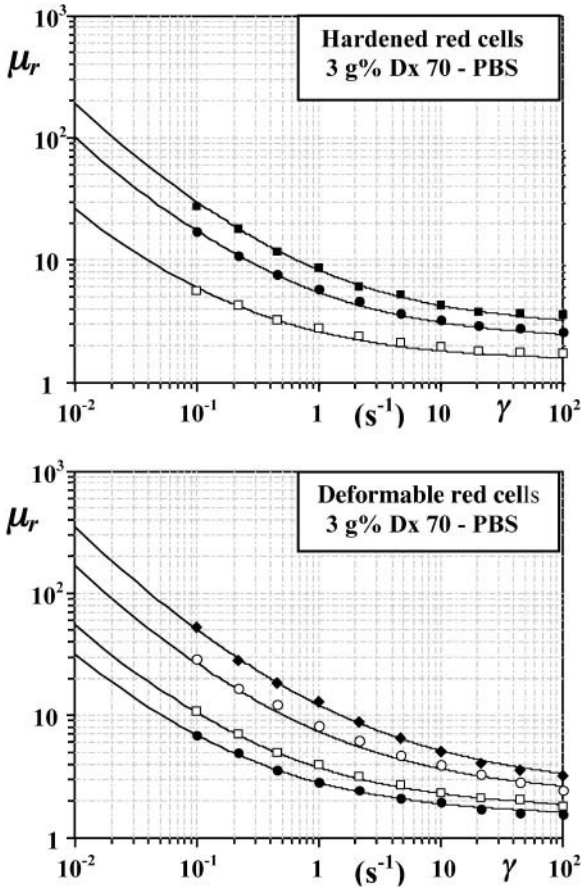

FIGURE 9 Shear rate dependence of the relative viscosity $\mu_r(\phi,\gamma) = \mu_a(\phi,\gamma)/\mu_o$for hardened (*top*) or deformable (*bottom*) red cells suspended in 3 g% dextran 70-PBS. Particle volume fraction (*top*) $\phi = 0.15$ (□), $\phi = 0.25$ (●), and $\phi = 0.3$ (■); (*bottom*) $\phi = 0.16$ (●), $\phi = 0.20$ (□), $\phi = 0.30$ (○), and $\phi = 0.35$ (♦). The solid curves were calculated from Eqs. 18–20, with an exponent $m = 1/2$, $D = 2$, $\beta = 0.3$, $\vartheta_o = 5.10^{-2}$ s, $\mu_i = 6$ cP, $\mu_o = 1.82$ mPa × s, and $\tau^* = 0.025$ N/m^2 (*top*) or $\tau^* = 0.028$ N/m^2 (*bottom*). The critical disaggregation shear stresses τ_c were determined from the rheo-acoustical method and $\phi_o^*(\phi)$ was derived from the low shear viscosity $\mu(\phi, \gamma \approx 0)$ of nonaggregated red cells.

CONCLUSION

In this work, a rheo-acoustical study was proposed to analyze the shear break-up processes of deformable or hardened red cell aggregates under well-defined hydrodynamic conditions. In addition the effective mean field approximation used in the microrheological models was examined on the basis of a fractal approach. The ultrasound scattering power from a dense distribution of reversible Rayleigh fractal clusters was found to be nearly isotropic. Far field coherence effects determine the cluster volume dependence of the scattering coefficient, without any dependence on the particle volume fraction or fractal dimension of the aggregates, because the ultrasonic wave cannot resolve the internal structure of aggregates smaller than a voxel $\approx \lambda/2\pi$ in size. The rheo-acoustical model for cluster break-up well

describes results of the ultrasonic experiments. The flow-dependent changes in the ultrasound scattered power from red cell clusters clearly establish the effective medium approximation used in the microrheological models. The shear stress dependence of the scattering cross-sectional area per unit of volume indicates that deformable or hardened red cell aggregates can be considered as soft clusters ($m = 1/2$) with a fractal dimension $D \approx 2$, and that they undergo irreversible deformation under the action of external stresses in relation with reversible flocculation.

Furthermore, the ultrasound scattering technique was found: i), suitable for determining the critical disaggregation shear stress of red cell suspensions; ii), representative of particle surface adhesive energy; and iii), to have the important advantage of being sensitive to cluster volume only, whatever the particle deformability and internal structure of the clusters. The critical disaggregation shear stress indeed exhibited no dependence upon membrane deformability after glutaraldehyde treatment of red cells. From the microrheological models based on a fractal approach and on measurements of disaggregation shear stresses, the shear thinning behavior of hardened or deformable red cell clusters is fairly well described in the low shear regime, because at low shear rates cell adhesiveness is weak and shear-induced restructuration processes are negligible.

Note, however, that the proposed rheo-acoustical model is no longer valid for clusters larger than a voxel, and ultrasound scattering becomes strongly anisotropic because of angle-dependent destructive interferences. In the fractal scattering regime, the dimensionless ultrasonic scattering coefficient involves the fractal dimension of the clusters and can no longer characterize the extent of particle aggregation.

REFERENCES

Angelson, B. A. J. 1980. A theoretical study of the scattering of ultrasound by blood. *IEEE Trans. Biomed. Eng.* 27:61–67.

Bascom, B. A. J., and R. S. C. Cobbold. 1995. On a fractal packing approach for understanding ultrasonic backscattering from blood. *J. Acoust. Soc. Am.* 98:3040–3049.

Boynard, M., and J. C. Lelievre. 1990. Size determination of red blood cell aggregates induced by dextran using ultrasound backscattering phenomenon. *Biorheology.* 27:39–46.

Chien, S., and K. M. Jan. 1975. Red cell aggregation by macromolecules. Roles of surface adsorption and electrostatic repulsion. *J. Supramol. Struct.* 1:385–409.

Cloutier, G., and Z. Qin. 1997. Ultrasound scattering from non-aggregating and aggregating erythrocytes: a review. *Biorheology.* 54:443–470.

Dunn, F., P. D. Edmonds, and W. J. Fry. 1969. Absorption and dispersion of ultrasound in biological media. *In* Biological Engineering. McGraw-Hill, New York, NY.

Fisher, M. E., and R. J. Burford. 1967. Theory of critical point scattering and correlations. The Ising model. *Physiol. Rev.* 156:583–592.

Greenleaf, J. F. 1996. Tissue Characterization with Ultrasound: Results and Applications, Vol. 11. CRC, Boca Raton, FL.

Greenleaf, J. F., and M. S. Chandra. 1992. *In* Biological System Evaluation with Ultrasound. Springer-Verlag, New York, NY.

Haider, L., P. Snabre, and M. Boynard. 2000. Rheo-acoustical study of the shear disruption of reversible aggregates. Ultrasound scattering from concentrated suspensions of red cell aggregates. *J. Acoust. Soc. Am.* 107:1715–1726.

Hanss, M., and M. Boynard. 1979. Ultrasound backscattering from blood: hematocrit and erythrocyte aggregation dependence. *In* Ultrasonic Tissue Characterization II (Spec. Pub. 525). M. Linzer, editor. National Bureau of Standard, Washington, D.C. 165–169.

Javanaud, C. 1989. The application of a fractal model to the scattering of ultrasound in biological media. *J. Acoust. Soc. Am.* 86:493–496.

Jullien, R., and R. Botet. 1987. Aggregation and Fractal Aggregates. World Scientific, Singapore.

Kolb, M., and R. Jullien. 1984. Chemically limited versus diffusion limited aggregation. *J. Phys. Lett.* 45:L977–L981.

Krieger, I. M. 1972. Rheology of monodisperse lattices. *Adv. Colloid Interface Sci.* 3:111–136.

Lin, M. Y., R. Klein, H. M. Lindsay, D. A. Weitz, R. C. Ball, and P. J. Meakin. 1990. The structure of fractal colloid aggregates of finite extent. *J. Colloid Interface Sci.* 137:263–280.

Lucas, R. J., and V. Twersky. 1987. Inversion of ultrasound scattering data from red blood cell suspensions under different flow conditions. *J. Acoust. Soc. Am.* 82:794–799.

Mills, P. 1985. Non Newtonian behavior of flocculated suspensions. *J. Phys. Lett.* 46:L301–L309.

Mills, P., and P. Snabre. 1988. The fractal concept in the rheology of concentrated suspensions. *Rheol. Acta.* 26:105–108.

Mo, L. Y. L., and R. S. C. Cobbold. 1992. A unified approach to modeling the backscattered Doppler ultrasound from blood. *IEEE Trans. Biomed. Eng.* 39:450–461.

Mo, L. Y. L., and R. S. C. Cobbold. 1993. Theoretical models of ultrasonic scattering in blood. *In* Ultrasonic Scattering in Biological Tissues. CRC Press, Boca Raton, FL. 125–171.

Neu, B., and H. J. Meiselman. 2002. Depletion-mediated red blood cell aggregation in polymer solutions. *Biophys. J.* 83:2482–2490.

Othmane, A., M. Bitbol, P. Snabre, and P. Mills. 1990. Influence of altered phospholipid composition of the membrane outer layer on red blood cell aggregation: relation to shape changes and glycocalyx structure. *Eur. Biophys. J.* 18:93–99.

Patel, P. D., and W. B. Russel. 1988. A mean field theory for the rheology of phase separated or flocculated dispersions. *Colloid Surf.* 31:355–383.

Potanin, A. A. 1993. On the computer simulation of the deformation and breakup of colloidal aggregates in shear flow. *J. Colloid Interface Sci.* 157:399–410.

Potanin, A. A., R. de Rooij, D. Van Den Ende, and J. Mellema. 1995. Microrheological modelling of weakly aggregated dispersions. *J. Chem. Phys.* 102:5845–5853.

Potanin, A. A., and N. B. Uriev. 1991. Microrheological models of aggregated suspensions in shear flow. *J. Colloid Interface Sci.* 142: 385–395.

Quemada, D. 1978. Rheology of concentrated dispersed systems. *Rheol Acta.* 17:632–642.

Quemada, D. 1998. Rheological modelling of complex fluids. I. The concept of effective volume fraction. *Eur. Phys. J. AP.* 1:119–127.

Quemada, D. 1999. Rheological modelling of complex fluids. IV. Thixotropic and thixoelastic behaviour. *Eur. Phys. J. AP.* 5:191–207.

Rayleigh, J. W. S. 1872. Investigation of the disturbance produced by a spherical obstacle on the waves of sound. *Proc. London Math Soc.* 4: 253.

Rayleigh, J. W. S. 1945. Vibrations of solid bodies. *In* Theory of Sound. Dover Publications, New York, NY. 414–431.

Shung, K. K., G. Cloutier, and C. C. Lim. 1992. The effects of hematocrit, shear rate and turbulence on ultrasonic Doppler spectrum from blood. *IEEE Trans. Biomed. Eng.* 39:462–469.

Shung, K. K., R. A. Sigelmann, and J. M. Reid. 1976. Scattering of ultrasound by blood. *IEEE Trans. Biomed. Eng.* 23:460–467.

Shung, K. K., and G. A. Thieme. 1993. Ultrasonic Scattering in Biological Tissue. CRC, Boca Raton.

Sigelmann, R. A., and J. M. Reid. 1973. Analysis and measurement of ultrasound backscattering from an ensemble of scatterers excited by sine-wave bursts. *J. Acoust. Soc. Am.* 53:1351–1355.

Skalak, R., P. R. Zarda, K. M. Jan, and S. Chien. 1981. Mechanics of rouleau formation. *Biophys. J.* 35:771–781.

Snabre, P. 1988. Rhéologie des suspensions concentrées et agrégées de particules déformables. Application à la suspension sanguine. State doctorate dissertation. University Paris VII, Paris, France.

Snabre, P., M. Bitbol, and P. Mills. 1987. Cell disaggregation behavior in shear flow. *Biophys. J.* 51:795–807.

Snabre, P., G. Grossamn, and P. Mills. 1985. Effects of dextran polydispersity on red blood cell aggregation. *Colloid Polym. Sci.* 263:478–483.

Snabre, P., L. Haider, and M. Boynard. 2000. Ultrasound and light scattering from a suspension of reversible fractal clusters in shear flow. *Eur. Phys. J. E.* 1:41–53.

Snabre, P., and P. Mills. 1996. Rheology of weakly flocculated suspensions of rigid particles I. Rheology of weakly flocculated suspensions of viscoelastic particles II. *J. Physique III.* 6:1811–1855.

Sonntag, R. C., and W. B. Russel. 1987. Structure and breakup of flocs subjected to fluid stresses. *J. Colloid Interface Sci.* 115:378–389.

Torres, F. R., W. B. Russel, and W. R. Schowalter. 1991. Simulations of coagulation in viscous flows. *J. Colloid Interface Sci.* 145:73–85.

Twersky, V. 1962. On scattering of waves by random distributions. I. Free space scatterer formalism. II. Two space formalism. *J. Math. Phys.* 3: 700–715; 724–734.

Twersky, V. 1978. Acoustic bulk parameters in distribution of pair-correlated scatterers. *J. Acoust. Soc. Am.* 36:1710–1719.

Twersky, V. 1987. Low-frequency scattering by correlated distributions of randomly oriented particles. *J. Acoust. Soc. Am.* 81:1609–1618.

Van Der Heiden, M. S., M. G. M. de Kroon, N. Bom, and C. Borst. 1995. Ultrasound backscatter at 30 MHz from human blood: influence of rouleau size affected by blood modification and shear rate. *Ultrasound Med. Biol.* 21:817–826.

Wessel, R., and R. Ball. 1992. Fractal aggregates and gels in shear flow. *Phys. Rev. A.* 46:R3008–R3011.

Wolthers, W., M. H. G. Duits, D. Van Den Ende, and J. Mellema. 1996. Shear history dependence of the viscosity of aggregated colloidal dispersions. *J. Rheol.* 40:799–811.

Yuan, Y. W., and Shung, K. K. 1988. Ultrasonic backscattering from flowing whole blood. II. Dependence on frequency and fibrinogen concentration. *J. Acoust. Soc. Am.* 84:1195–1200.